International Journal of Pharmaceutics 382 (2009) 165–171

Contents lists available at ScienceDirect

International Journal of Pharmaceutics

journal homepage: www.elsevier.com/locate/ijpharm

A drug-in-adhesive transdermal patch for *S*-amlodipine free base: *In vitro* and *in vivo* characterization

Yinghua Sun[a], Liang Fang[a,*], Meng Zhu[a], Wei Li[a], Ping Meng[a], Li Li[b], Zhonggui He[a]

[a] *School of Pharmacy, Shenyang Pharmaceutical University, Shenyang, Liaoning 110016, China*
[b] *School of Pharmaceutical Sciences, Liaoning University, Shenyang, Liaoning 110036, China*

ARTICLE INFO

Article history:
Received 27 May 2009
Received in revised form 24 July 2009
Accepted 23 August 2009
Available online 28 August 2009

Keywords:
Drug-in-adhesive transdermal patch
S-amlodipine
Rat
Pharmacokinetics

ABSTRACT

The objective of the present investigation was to develop and evaluate a drug-in-adhesive transdermal patch for *S*-amlodipine (*S*-AM) free base. Initial *in vitro* experiments were conducted to optimize the formulation parameters before transdermal delivery in rats. The effects of the type of adhesive and the content of permeation enhancers on *S*-AM free base transport across excised rat skin were evaluated. For *in vivo* studies, patches were administered transdermally to rats while orally administered *S*-AM in suspension and intravenously administered *S*-AM solution were used as controls. The plasma level of *S*-AM following transdermal application could be maintained for 72 h. After transdermal administration to rats, the absolute bioavailability was 88.8% for *S*-AM free base. After dose normalization, the areas under the plasma concentration–time curve (AUC) and mean residence times (MRT) were evidently increased and extended, respectively. This suggests that the transdermal application of *S*-AM in a drug-in-adhesive transdermal patch may be used for the treatment for hypertension.

1. Introduction

Amlodipine, a third-generation dihydropyridine calcium channel antagonist, is prescribed for the management of angina and hypertension. Essentially, the calcium channel-blocking effect is confined to the *S*-amlodipine (*S*-AM) isomer (Goldmann et al., 1992), whereas *R*-amlodipine exhibits a much lower calcium channel-blocking activity (3 orders of magnitude) (Zhang et al., 2002). Considering that only *S*-AM (Fig. 1) possesses the desired activity, the successful development of an amlodipine formulation consisting of only *S*-AM is an attractive option.

Patients suffering from these diseases usually require long-term medication and patient compliance is very important. The daily dose of *S*-AM ranges from 2.5 to 5 mg, which is very suitable for transdermal therapeutic systems (TTS).

Francoeur and Potts (1988) have reported the feasibility of developing an effective transdermal system for amlodipine besylate (AM-B). McDaid and Deasy (1996) have discussed the formulation development of a reservoir-type transdermal system using amlodipine. However, the steady-state flux they obtained needs further improvement in order to attain the clinical levels required in patients. In addition, we have recently investigated *in vitro* percutaneous absorption of racemic amlodipine free base and its complexes through excised rat skin using 2-chamber diffusion cells. The results obtained showed that racemic amlodipine free base had the greatest steady-state flux and lowest permeability coefficient of the five compounds from the EI system (ethanol:IPM = 2:8), and its four complexes all exhibited a lower flux and higher permeability coefficient than racemic amlodipine (Jiang et al., 2008).

Among the different types of systems, the drug-in-adhesive products, in which the drug is included in the adhesive layer in contact with the skin, are very commonly used, being thin and comfortable to wear.

The aim of the present study was to investigate *S*-AM transport from a transdermal patch system. The effect of the type of adhesive and the content of permeation enhancers on *S*-AM transport across the rat skin were evaluated. For *in vivo* studies, the patch pharmacokinetics were evaluated by comparing the pharmacokinetic profile of a transdermal system with that of an intravenous one and two oral forms in rats.

2. Materials and methods

2.1. Materials

S-Amlodipine besylate (*S*-AM-B) was purchased from Jilin Tianfeng Pharmaceutical Co., Ltd. (Jilin, China); isopropyl myristate (IPM) and l-menthol were supplied by China National Medicines Co., Ltd. (Shanghai, China); acetic ether and polyethylene glycol 400 (PEG400) were obtained from the Bodi Drug Manufacturing Co., Ltd. (Tianjin, China). DURO-TAK® adhesives 87-2677

* Corresponding author. Tel.: +86 24 23986330; fax: +86 24 23986330.
E-mail address: fangliang2003@yahoo.com (L. Fang).

0378-5173/$ – see front matter © 2009 Elsevier B.V. All rights reserved.
doi:10.1016/j.ijpharm.2009.08.031

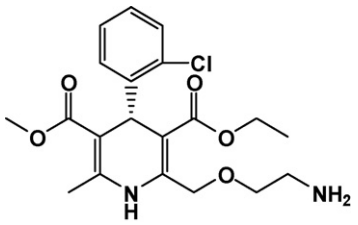

Fig. 1. The chemical structure of *S*-amlodipine.

(chemical composition: acrylate), 87-4098 (chemical composition: acrylate–vinylacetate) and 87-9301 (chemical composition: acrylate) were gifts from the National Starch and Chemical Company (Bridgewater, NJ, USA). Methanol of HPLC grade was obtained from the Yuwang Pharmaceutical Co., Ltd. (Shandong, China). Acetonitrile of HPLC grade was purchased from Fisher Scientific (Fairlawn, NJ, USA). All other chemicals and solvents were of analytical reagent grade.

2.2. Preparation of S-AM

2.2.1. Preparation of S-AM

S-AM was prepared from *S*-AM-B, which was available on the market. *S*-AM-B was dissolved in 20% methanol solution (approximately 20 mg/ml) at 50 °C. The pH of the solution was adjusted to 11 using 1.0 mol/l sodium hydroxide solution then it was extracted into acetic ether. Anhydrous sodium sulfate was added to the organic solution in order to eliminate residual water. The acetic ether extracts were filtered and evaporated using a rotary vacuum evaporator. The residue was dried to the state of viscous yellow oil, which eventually crystallized after storage at 4 °C.

2.2.2. DSC

DSC measurements were performed using a Shimadzu DSC-60 thermal analyzer. Samples were placed in a standard aluminium crucible fitted with a perforated lid for scanning. An empty pan was used as a reference. The samples were heated at a rate of 5 °C min^{-1} over a temperature range of 20–250 °C.

2.3. Formulations

Appropriate amounts of pressure-sensitive adhesive, *S*-AM (4%, w/w) and penetration enhancers were added to acetic ether on a weight basis, then agitated at room temperature for 60 min. The mixture was applied to the surface of a fluoropolymer-treated polyester release liner (ScotchPak® 1022, 3M, USA) kept in a static state for 20 min, and dried at 60 °C for 10 min. After cooling, the patches were cut, covered with a polyester backing membrane (ScotchPak® 9726, 3M, USA), and placed in an aluminium–plastic membrane.

2.4. S-AM in vitro permeation profile through rat skin

Male Wistar rats weighing 180–220 g (6–8 weeks old) used in all experiments were supplied by the Experimental Animal Center of Shenyang Pharmaceutical University (Shenyang, China). The study was conducted in accordance with the Ethical Guidelines for Investigations in Laboratory Animals and was approved by the Ethics Review Committee for Animal Experimentation of Shenyang Pharmaceutical University. All efforts were made to minimize animal suffering and to limit the number of animals used.

The rats were anesthetized with urethane (20%, w/v i.p.) and the abdomen carefully shaved with a razor after removal of hair by electric clippers (model 900, TGC, Japan). After sacrificing the rats by dislocating the spinal cord, a sample of full thickness skin (i.e. epidermis with stratum corneum and dermis) was excised from the shaved abdominal site. The integrity of the skin was carefully checked by microscope observation, and any skin which had poor uniformity was rejected. After removing the fat and subdermal tissue, the skin was kept frozen at −20 °C and used within 1 week. Before starting the experiment, it was allowed to reach room temperature for at least 10 h.

Skin permeation studies were performed using a two-chamber side-by-side glass diffusion cell equipped with star-head magnetic stirrers and a water jacket. Each half-cell had a volume of 2.5 ml and an effective diffusion area of 0.95 cm^2. The excised abdominal skin was mounted between the cell halves so that the dermal side of the skin faced the receiver fluid. A circular transdermal patch was pressed on the skin with the adhesive side facing the stratum corneum (SC). After securely clamping the cell assembly together, the receptor compartment was filled with 2.5 ml pH 7.4 phosphate buffer solution (PBS) containing 40% (v/v) PEG400 (40% PEG400 PBS) to maintain sink conditions and continuously stirred at about 600 rpm. The temperature of the cell was maintained at 32 ± 1 °C using thermostatically controlled water which was circulated through a water jacket surrounding the cell body throughout the experiments. Care was taken to ensure that no air bubbles remained in the water jacket. At predetermined time intervals, 2.0 ml of receptor solution was taken for analysis and replaced with the same volume of fresh solution to maintain sink conditions.

The samples were centrifuged for 5 min at 1600 rev/min and an aliquot of 20 μl of supernatant was analyzed by HPLC to determine the drug content. Experiments were replicated at least four times.

2.5. In vivo studies

2.5.1. In vivo studies in rats

Male Wistar rats were used after being allowed to acclimatize for 1 week. Eighteen 200–240 g (8–10 weeks old) rats were used in the study. Before administration, rats were fasted overnight but were allowed access to water. Rats were divided into three equal groups (6 animals each): groups A, B and C. The weight of the animals was measured and recorded before the start of each experiment.

Thereafter, the rats in group A were given an intravenous administration of *S*-AM 2 mg/kg (dissolved in 10% alcohol solution (1 mg/ml)) via the tail vein. Six rats in group B were given intragastric doses of *S*-AM suspension (0.5 mg/ml in 0.5% (w/v) CMC-Na) 2 mg/kg twice (the second time was 24 h immediately after collection of the blood sample). On the day before the start of the experiment, the test areas on the abdominal site of the rats in group C were shaved without damaging the skin. Prior to the application of the test medication, the skin was cleaned carefully with warm water followed by an alcohol swab and patted dry to avoid any adhesion problems caused by residues on the skin. The animals in the patch group were treated with an *S*-AM transdermal patch in a randomized order, and the patch was removed after an interval of 48 h. A single patch with an area of about 5 cm^2 and containing 5.0 mg *S*-AM was applied to the shaved skin.

Blood samples of 0.1–0.2 ml were collected from the jugular vein and placed in dried heparinized tubes at 0.083, 0.167, 0.333, 0.5, 1, 1.5, 2, 3, 4, 6, 8, 12 and 24 h after i.v. administration, 2, 4, 6, 8, 10, 12, 24, 26, 28, 30, 32, 36, 48 and 60 h after oral administration and 1, 6, 12, 24, 30, 36, 48, 60, 72, 84 and 96 h after transdermal administration.

Plasma samples were separated immediately by centrifugation at 3000 rev/min for 10 min, and stored at −20 °C until analysis.

2.6. Plasma sample preparation

To a 50 μl aliquot of plasma in 5 ml conical centrifuge tubes, 50 μl internal standard (40 ng/ml) and 50 μl acetonitrile:water

(40:60, v/v) were added. The samples were vortexed for 30 s and 3 ml diethyl ether was added. The mixture was then vortex-mixed for 3 min. After centrifugation at 3500 × *g* for 10 min, the upper organic layer was transferred to another set of clean glass tubes and evaporated to dryness at 40 °C under a gentle stream of nitrogen. The residue was reconstituted in 100 μl acetonitrile: water (40:60, v/v), and transferred to glass vials, and an aliquot of 5 μl was injected into the UPLC–MS/MS system for analysis.

2.7. Analytical methods

2.7.1. In vitro quantitative analysis

The concentrations of *S*-AM were measured by HPLC. The HPLC equipment consisted of a HITACHI L7110 pump, a HITACHI UV–VIS L-7420 detector (both from Hitachi High-Technologies Corporation, Tokyo, Japan), and an HT-220A column temperature controller (Tianjin, China). Analyses were performed on a 5-μm ODS column (200 mm × 4.6 mm, DIKMA technologies, Beijing, China) operated at 40 °C. The mobile phase was methanol-0.03 mol/l KH_2PO_4 buffer solution (7:3) at a flow rate of 1 ml/min. The wavelength of the detector was 238 nm and the internal standard was 8 μg/ml propylparaben. Calibration curves were constructed using the peak area ratio of *S*-AM and propylparaben *versus* the concentration of *S*-AM in solution. The retention times of the drug and the internal standard were approximately 4.3 and 5.8 min, respectively. The retention time of the main impurity of *S*-AM was 9.3 min.

2.7.2. In vivo quantitative analysis

2.7.2.1. Liquid chromatography. Liquid chromatography was performed on an ACQUITY™ UPLC system (Waters Corp., Milford, MA, USA) with cooling in an auto-sampler and a column oven to enable temperature control of the analytical column. An ACQUITY UPLC™ BEH C_{18} column (50 mm × 2.1 mm, 1.7 μm; Waters Corp., Milford, MA, USA) was employed. The column temperature was maintained at 45 °C and the mobile phase was 40% acetonitrile and 60% water containing 0.2% formic acid. The flow rate was set at 0.2 ml/min. The auto-sampler was conditioned at 4 °C and the injection volume was 5 μl using the partial loop mode for sample injection.

2.7.2.2. Mass spectrometry. Triple-quadrupole tandem mass spectrometric detection was carried out on a Micromass® Quattro micro™ API mass spectrometer (Waters Corp., Milford, MA, USA) with an electrospray ionization (ESI) interface. The ESI source was operated in positive ionization mode. Quantification was performed using multiple reaction monitoring (MRM) of the transitions of *m*/*z* 409 → 238 for *S*-AM and *m*/*z* 260 → 116 for propranolol (the internal standard), respectively, with a scan time of 0.2 s per transition. The optimal MS parameters obtained were as follows: capillary 3.0 kV, cone 20 kV, source temperature 120 °C and desolvation temperature 350 °C. Nitrogen was used as the desolvation and cone gas with a flow rate of 550 and 50 l/h, respectively. Argon was used as the collision gas at a pressure of approximately 3.53×10^{-3} mbar. All data were processed using MassLynx™ NT 4.0 software with a QuanLynx™ program (Waters Corp., Milford, MA, USA).

2.8. Statistical analysis

2.8.1. Data analysis in vitro

The amount of drug that had penetrated at each sampling interval was obtained from the measured concentration and volume of the receiver phase. The cumulative amount of drug was calculated by the following formula:

$$Q = \frac{\sum_{i=2}^{n}(2.5C_i - 0.5C_{i-2})}{A} \quad i = 2, 4, 6 \ldots$$

where Q is the cumulative amount penetrated; C_i is the concentration in the receiver compartment at time i; and A is the effective diffusion area (0.95 cm^2). The cumulative amount penetrated from unit area *versus* time was plotted. The steady-state flux (J_s) was calculated from the slope of the linear portion of the plotted curve. The lag-time (t_{lag}) was the intercept obtained by extrapolation of the linear portion to the time axis. For comparison of two groups of data, significance was determined by Student's *t*-test. Data were considered significant at a *p*-value of <0.05.

2.8.2. In vivo pharmacokinetic analysis

Pharmacokinetic parameters, such as the maximal plasma drug concentration (C_{max}) and time to maximal plasma drug concentration (T_{max}), were read directly from the individual blood concentration–time profiles. The AUC_{0-t} (area under the time concentration curve from time 0 to time t) was calculated by the linear trapezoidal rule. The half-life of elimination from plasma ($t_{1/2}$) was determined by linear regression of the terminal portion of the log plasma concentration *versus* time curves, and the mean residence time (MRT) values were obtained by non-compartmental analyses.

Absolute bioavailability (F) was calculated from the following equation:

$$F = \frac{AUC_{transdermal}}{AUC_{i.v.}} \times \frac{dose_{i.v.}}{dose_{transdermal}}$$

The steady-state plasma concentration of *S*-AM after the application of patches was calculated from the equation (Valiverti et al., 2005): $C_{ss} = AUC_{0-t}/time$, time is 48 h (the application of *S*-AM transdermal patches was for a 48 h period).

Data are expressed as the mean ± standard deviation (S.D.).

3. Results and discussion

3.1. Preparation of S-AM from S-AM-B

S-AM free base was prepared from *S*-AM-B available commercially. The yield could be over 85%. The prepared product was identified as highly pure (>99.5%) by the area normalization method of HPLC. The DSC curves of *S*-AM exhibited characteristic sharp endothermic peaks corresponding to its melting point (109.27 °C). Fig. 2 shows the DSC curves of AM, AM-B, *S*-AM and *S*-AM-B at a heating rate of 5 °C/min over the experimental temperature range of 20–250 °C. Table 1 summarizes the melting points and the enthalpies of fusion for AM, AM-B, *S*-AM and *S*-AM-B.

3.2. The cumulative permeation profiles of S-AM from transdermal patches

The rank order of the melting points is as follows: *S*-AM-B < *S*-AM < AM. The melting point of *S*-AM-B is lower than that of *S*-AM, but its molecules is higher (MW > 500). The melting point may also be considered as an important predictor of skin permeability as it correlates strongly with the oil solubility of drugs (Barratt, 1995). We investigated the *in vitro* percutaneous absorption of *S*-AM-B and *S*-AM at the same molar concentration in 87-9301 adhesive patches without penetration enhancers. Comparing the penetration results,

Table 1
DSC melting characteristics of AM, AM-B, *S*-AM and *S*-AM-B.

	M.p. (°C)	Enthalpy of fusion (kJ/mol)
AM	142.32	25.79
AM-B	200.41	33.59
S-AM	70.46	23.03
S-AM-B	109.27	34.20

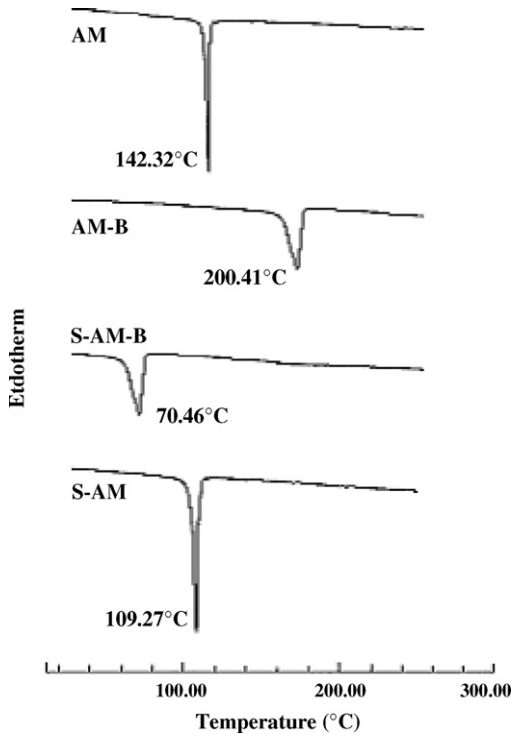

Fig. 2. DSC curves of AM, AM-B, *S*-AM and *S*-AM-B at a heating rate of 5 °C/min.

S-AM-B exhibited a lower flux than *S*-AM ($0.19 \pm 0.06\ \mu g\ h^{-1}\ cm^{-2}$ *versus* $2.41 \pm 0.32\ \mu g\ h^{-1}\ cm^{-2}$). The result obtained showed that *S*-AM-B is not a candidate for passive transdermal delivery which confirmed the hypothesis that the lipophilic free base of *S*-AM has better properties than the hydrophilic salt in terms of skin permeation.

As a base for the adhesive layer of the adhesive patch, it is important in screening a formulation for a transdermal drug delivery system to choose a suitable adhesive. Duro-Tak® acryl adhesives were selected and evaluated for the *in vitro* rat skin permeation studies.

The thickness of the patches was measured with a micrometer and was calculated by subtracting the combined thickness of the backing membrane and release liner from the thickness of the whole patch. The thickness of all the patches used was $70 \pm 10\ \mu m$.

The cumulative permeation profiles of *S*-AM from the three different adhesives are shown in Fig. 3. A steady and continuous permeation of *S*-AM from all the patches was observed, indicating that *S*-AM was dissolved in all the adhesives with a uniform distribution.

The permeation parameters of *S*-AM with different adhesives containing 4% *S*-AM in patches through excised rat skin are shown in Table 2. These results illustrate that 87-9301 is an ideal adhesive for the development of *S*-AM transdermal patches.

In the adhesive layer of the adhesive patch, penetration enhancers may be used to reduce the barrier properties of the SC. Such penetration enhancers may be used alone, or as a mixture of two or more. Further studies were conducted by preparing 87-9301 adhesive patches with different proportions of penetration enhancers.

Table 3 shows the permeation parameters of *S*-AM from the patches containing 4% *S*-AM and the enhancers in 87-9301. At a concentration of 7%, the cumulative amount *S*-AM permeated was the highest. The maximum flux attained with 7% IPM was $13.99 \pm 1.85\ \mu g\ h^{-1}\ cm^{-2}$. The permeation-enhancing effect of IPM was confirmed by the *in vitro* skin permeation study. An enhancement ratio of 5.16 was observed when *S*-AM was delivered from the formulation containing IPM as compared with the formulation without IPM. This can be explained by the fact that the solubility parameter of IPM ($16.40\ MPa^{1/2}$) is similar to that of skin ($20.01\ MPa^{1/2}$), which leads to a high affinity of IPM for SC. The high affinity of IPM for SC may result in formation of a pool and the pool of IPM could drive the drug eventually into the SC, thereby reducing the SC barrier function (Panchagnula et al., 2005).

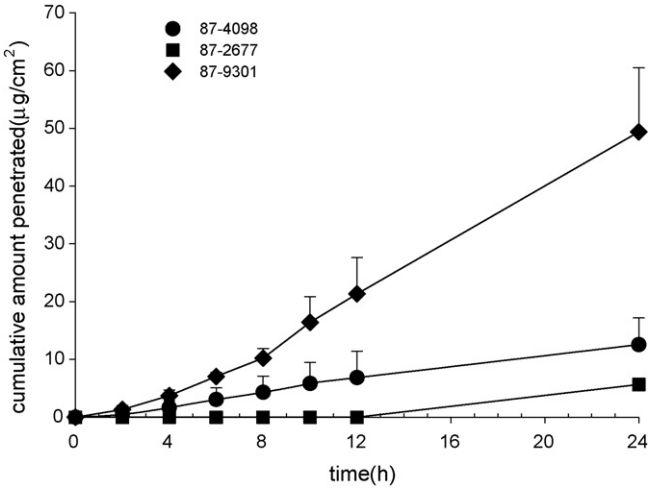

Fig. 3. The penetration profiles of *S*-AM patches in the presence of different adhesives. Data are presented as the mean ± standard deviation (S.D.).

An obvious increase in the permeation of *S*-AM was found following the binary combinations of l-menthol and IPM which indicates that l-menthol acts synergistically with IPM. Meanwhile, the l-menthol stabilizes mainly in the central region of the SC membranes attracting the membrane lipids and causing hydrogen bond ruptures in the polar membrane interface (dos Anjos et al., 2007). Also, 7% l-menthol in addition to 7% IPM had the greatest enhancing effect in terms of the accumulated amount permeated, but the formation of the crystallisation in the adhesive matrix was observable visually as well as by optical microscopy (DMBA 450, Motic China Group Co., Ltd., China) after a few days (Fig. 4). These findings demonstrated that such a system was unstable and the compatibility between this kind of adhesive and l-menthol was poor.

For the above reason, the final formulation contained 3.5% l-menthol and 7% IPM as penetration enhancers. The patches were smooth, uniform and flexible. A steady-state skin permeation rate of $16.10 \pm 1.87\ \mu g\ h^{-1}\ cm^{-2}$ was achieved after an initial lag-time of 5.25 ± 0.79 h.

Table 2
The permeation parameters of *S*-AM with different adhesives containing 4% *S*-AM in patches through excised rat skin ($n = 3$, mean ± S.D.).

	J_s ($\mu g\ h^{-1}\ cm^{-2}$)	Q_{24} ($\mu g\ cm^{-2}$)	t_{lag} (h)
87-4098	0.65 ± 0.31	12.25 ± 4.66	1.25 ± 0.12
87-2677	0.45 ± 0.02	5.67 ± 0.60	11.89 ± 0.16
87-9301	2.41 ± 0.32	49.39 ± 11.09	3.39 ± 0.78

Table 3
The permeation parameters of *S*-AM through excised rat skin from the patches containing 4% *S*-AM and the enhancers in 87-9301 ($n = 3$, mean ± S.D.).

Enhancer(s)	J_s ($\mu g\ h^{-1}\ cm^{-2}$)	Q_{24} ($\mu g\ cm^{-2}$)	t_{lag} (h)
3.5% IPM	7.25 ± 1.77	141.44 ± 39.99	4.70 ± 1.48
7% IPM	11.52 ± 1.55	254.69 ± 65.42	4.58 ± 1.00
7% IPM:3.5% l-menthol	16.10 ± 1.87	295.74 ± 37.56	5.25 ± 0.79
7% IPM:7% l-menthol	18.46 ± 3.45	368.70 ± 89.56	1.66 ± 0.84

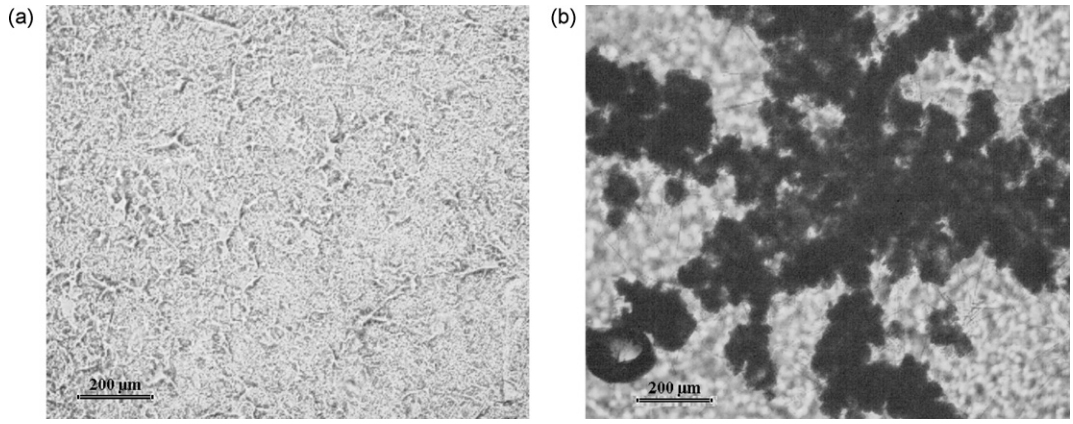

Fig. 4. The optical microscopy of *S*-AM transdermal patch containing 7% l-menthol and 7% IPM as penetration enhancers, storage at room temperature: (a) 1 day and (b) 2 weeks.

3.3. Pharmacokinetics study

3.3.1. Concentration–time profiles

The mean plasma concentration–time profiles of *S*-AM after intravenous injection, oral and transdermal administration are shown in Fig. 5.

After intravenous (i.v.) injection of *S*-AM 2 mg/kg (dissolved in 10% alcohol solution (1 mg/ml)) via the tail vein, the mean plasma concentration was minimal at 24 h.

The results for the oral administration of *S*-AM indicated that it was rapidly absorbed from the gastrointestinal tract with a C_{max} of $24.33 \pm 9.47\ ng\ ml^{-1}$ at a T_{max} of 6.00 ± 1.26 h after the first administration, and with a C_{max} of $21.31 \pm 9.90\ ng\ ml^{-1}$ at a T_{max} of 5.67 ± 1.51 h after the second administration, and became minimal at 60 h.

Transdermal administration of *S*-AM achieved a C_{max} of $160.47 \pm 19.16\ ng\ ml^{-1}$ at a T_{max} of 32.00 ± 2.83 h, and was minimal at 96.0 h. The whole blood concentration of *S*-AM declined more slowly than that following oral administration.

It was noted that the C_{max} after oral administration persisted for a short period and then the plasma drug concentration continued to decline while, in the case of transdermal administration, it was maintained for almost 48 h.

Furthermore, it was observed that there were no significant changes in the skin surface after removal of the *S*-AM transdermal patch.

Upon removal of the transdermal patch, a mild reservoir effect was observed for about 48 h followed by normal elimination similar to that after oral administration.

3.3.2. Pharmacokinetic parameters

The pharmacokinetic parameters of *S*-AM are presented in Table 4. Compared with two oral administrations without dose normalization, the AUC_{0-t} values were significantly increased: $6964.5 \pm 307.9\ h\ ng\ ml^{-1}$ for *S*-AM transdermally *versus* $627.70 \pm 130.47\ h\ ng\ ml^{-1}$ for *S*-AM intravenously, and the MRT values were clearly prolonged: 37.61 ± 3.30 h for *S*-AM transdermally *versus* 11.02 ± 2.25 h for *S*-AM orally, and 8.50 ± 1.07 h for *S*-AM intravenously, respectively.

Similarly, the apparent $t_{1/2}$ values were also markedly increased: 12.38 ± 1.84 h for *S*-AM transdermally *versus* 4.60 ± 0.87 h for *S*-AM orally, 6.74 ± 0.86 h for *S*-AM intravenously.

After dose normalization, the absolute bioavailability of transdermal administration was 88.8%, while that of oral administration was 37.2% for *S*-AM.

The pharmacokinetic study indicates that the concentration of *S*-AM after transdermal administration of one patch persists for at least 3 days while the drug orally administered once daily produced obvious fluctuations in plasma concentration during the dosage interval.

The pharmacokinetic profile of *S*-AM has been reported in rats (2 mg/kg i.v. and 8 mg/kg p.o.) (Stopher et al., 1988). After oral administration of the *S*-AM suspension, 2 mg/kg twice, the absolute bioavailability was much lower than that in the previous report (37.2% for the present study *versus* 100%, both in rats). This may be due to one reason: the difference in the administration dosage (2 mg/kg p.o. *versus* 8 mg/kg p.o.). The calculated plasma clearance ($54.86 \pm 10.27\ ml\ min^{-1}\ kg^{-1}$) which is close to the liver blood flow ($60\ ml\ min^{-1}\ kg^{-1}$) in this species (Lave et al., 1997) is reasonable compared with the calculated result reported in the literature. This result in the literature may indicate dose-dependent kinetics in the rat, with first-pass metabolism being saturated after an oral dose of 8 mg/kg (four times the i.v. dose). There is no report about the transdermal patch of *S*-AM. The high absolute bioavailability of *S*-AM in this study shows that *S*-AM is fully absorbed into the systemic circulation after transdermal administration.

In addition, the half-life of elimination from plasma ($t_{1/2}$) and the maximal plasma drug concentration (C_{max}) of *S*-AM given orally to rats were comparable with the reported value of *S*-AM after oral dosage of AM (20 mg/kg) at 10 a.m. in rats (Fujimura et al., 1993).

After transdermal administration, the MRT of *S*-AM was prolonged compared with that after oral administration. This may be due to the longer duration of absorption provided by the transdermal patch. Also, prolonged duration of action is possible with a single application of a transdermal patch.

The T_{max} of *S*-AM given orally to rats is close to the reported value following oral administration to humans (6 h), while there is an obvious difference in $t_{1/2}$ between rats and humans: 55 h in

Table 4
Pharmacokinetic parameters of *S*-AM after two (the second time is 24 h immediately after the blood sample was collected) oral administrations of *S*-AM suspension (0.5 mg/ml in 0.5% (w/v) CMC-Na) 2 mg/kg, transdermal administration as a single patch (containing *S*-AM 5.0 mg, and the patch was removed from the rat after an interval of 48 h) and intravenous injection of *S*-AM 2 mg/kg (dissolved in 10% alcohol solution (1 mg/ml)) via the tail vein ($n = 6$).

	Transdermal	Oral	i.v.
C_{max1} (ng/ml)	160.47 ± 19.16	24.33 ± 9.47	
T_{max1} (h)	32.00 ± 2.83	6.00 ± 1.26	
C_{max2} (ng/ml)		21.31 ± 9.90	
T_{max2} (h)		5.67 ± 1.51	
AUC_{0-t} ($h\ ng\ ml^{-1}$)	6964.5 ± 307.9	467.2 ± 87.01	627.7 ± 130.47
MRT (h)	37.61 ± 3.30	11.02 ± 2.25	8.50 ± 1.07
Cl ($ml\ min^{-1}\ kg^{-1}$)			54.86 ± 10.27
$T_{1/2}$ (h)	12.38 ± 1.84	4.60 ± 0.87	6.74 ± 0.86

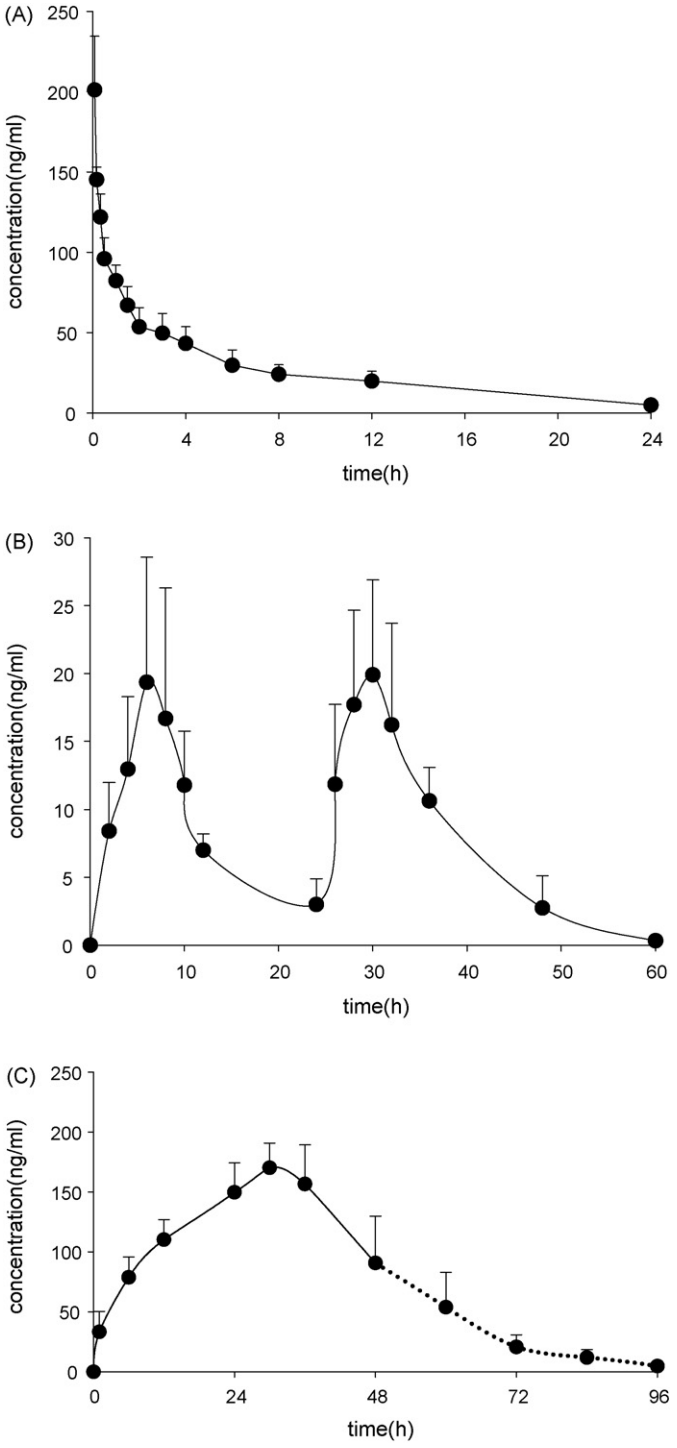

Fig. 5. Plasma concentration–time profiles of *S*-AM after intravenous (i.v.) injection of *S*-AM 2 mg/kg (dissolved in 10% alcohol solution (1 mg/ml)) via the tail vein (group A, $n = 6$), oral administration of *S*-AM suspension (0.5 mg/ml in 0.5% (w/v) CMC-Na) 2 mg/kg twice (the second time was 24 h immediately after collection of the blood sample) (group B, $n = 6$) or *S*-AM transdermal patch (the patch was removed after an interval of 48 h) (group C, $n = 6$). (A) Mean plasma concentration–time profile after i.v. injection; (B) mean plasma concentration–time profile after two oral administrations of *S*-AM suspension; (C) mean plasma concentration–time profile after transdermal administration. The dotted line (. . .) indicates the plasma concentration after the removal of the patches. Data are presented as the mean ± standard deviation (S.D.)

men and 5 h in rats. Pharmacodynamic assessment in that report showed that the systolic blood pressure (SBP), diastolic blood pressure (DBP), and heart rate (HR) changed significantly during the 4–10 h period following the administration 5 mg *S*-AM. This indicates that the drug maintains its anti-hypertensive efficacy only for about 6 h near the T_{max} of *S*-AM given orally once daily. The pharmacokinetic profile of oral *S*-AM indicates that the whole blood concentration of *S*-AM declined rapidly and, hence, produced a shorter duration of therapeutic action (Park et al., 2006).

Compared with oral administration, the transdermal preparation of *S*-AM resulted in a prolonged T_{max}. The sustained response following transdermal administration was due to controlled and continuous release of drug into the systemic circulation over an extended period. Therefore, the transdermal route for *S*-AM is a better alternative to avoid hepatic first-pass metabolism and to achieve a constant plasma level over an extended period of time, which additionally requires less frequent dosing. The drug incorporated in the adhesive patch is percutaneously absorbed and exhibits sufficient drug efficacy.

3.4. In vitro/in vivo correlation

The simulated steady-state concentration was calculated from the following equation (Tenjarla et al., 1994):

$$\text{I.R.} = C_{ss} \cdot \text{Cl} = J_s \cdot A$$

This is the mass balance equation at steady-state, where I.R. is the input rate into the body through the skin, C_{SS} is the steady-state plasma concentration (ng ml^{-1}); J_s is the steady-state *S*-AM flux from the patch; A is area of the applied patch (5 cm^2); and Cl is the total body clearance of 54.86 ml min^{-1} kg^{-1} determined from the intravenous pharmacokinetic study.

The observed *in vivo* steady-state plasma concentration 115.9 ng ml^{-1} after transdermal administration in rats is in good agreement with the simulated steady-state concentration of 122.3 ng ml^{-1}. This indicates that the *in vitro* experiment with rat skin may be used for further transdermal drug delivery studies with *S*-AM since there is a great similarity between the simulated and *in vivo* steady-state concentration.

4. Conclusions

In conclusion, the present data confirm the feasibility of developing an *S*-AM transdermal patch to provide plasma levels for 3 days in rats. A selective and rapid specific UPLC–MS–MS method was developed for the quantitation of *S*-AM in rat plasma. Compared with oral *S*-AM administration, the transdermal route for *S*-AM is a better alternative to avoid hepatic first-pass metabolism and to achieve a constant plasma level over an extended period of time. The correlation analysis revealed that the *in vitro* skin permeation data in rats could underestimate the true permeability of *S*-AM *in vivo*.

Further work is needed to allow the pharmacodynamic assessment of the transdermal patch and refine it in order to attain suitable clinical levels in patients.

Acknowledgement

The authors wish to thank Professor Yasunori Morimoto, Faculty of Pharmaceutical Sciences, Josai University, Japan, for providing the 2-chamber diffusion cells.

References

Barratt, M.D., 1995. Quantitative structure-activity relationships for skin permeability. Toxic. In Vitro 9, 27–37.

dos Anjos, J.L., de Sousa Neto, D., Alonso, A., 2007. Effects of ethanol/l-menthol on the dynamics and partitioning of spin-labeled lipids in the stratum corneum. Eur. J. Pharm. Biopharm. 67, 406–412.
Francoeur, M.L., Potts, R.O., 1988. Transdermal flux enhancing compositions. EP Patent Application 0271983, 22 June.
Fujimura, A., Shiga, T., Ohashi, K., Ebihara, A., 1993. Chronopharmacology of amlodipine in rats. Life Sci. 53, 595–602.
Goldmann, S., Stoltefuss, J., Born, L., 1992. Determination of the absolute configuration of the active amlodipine enantiomer as (−)-S: A correction. J. Med. Chem. 35, 3341–3344.
Jiang, Y., Fang, L., Niu, X., Rui, M., He, Z., 2008. The effect of ion pairing on the skin permeation of amlodipine. Pharmazie 63, 356–360.
Lave, T., Dupin, S., Schmitt, C., Chou, R.C., Jaeck, D., Coassolo, P., 1997. Integration of *in vitro* data into allometric scaling to predict hepatic metabolic clearance in man: application to 10 extensively metabolized drugs. J. Pharm. Sci. 86, 584–590.
McDaid, D.M., Deasy, P.B., 1996. Formulation development of a transdermal drug delivery system for amlodipine base. Int. J. Pharm. 133, 71–83.
Panchagnula, R., Desu, H., Jain, A., Khandavilli, S., 2005. Feasibility studies of dermal delivery of paclitaxel with binary combinations of ethanol and isopropyl myristate: role of solubility, partitioning and lipid bilayer perturbation. Farmaco 60, 894–899.
Park, J.Y., Kim, K.A., Park, P.W., Lee, O.J., Ryu, J.H., Lee, G.H., Ha, M.C., Kim, J.S., Kang, S.W., Lee, K.R., 2006. Pharmacokinetic and pharmacodynamic characteristics of a new *S*-amlodipine formulation in healthy Korean male subjects: a randomized, open-label, two-period, comparative, crossover study. Clin. Ther. 28, 1837–1847.
Stopher, D.A., Beresford, A.P., Macrae, P.V., Humphrey, M.J., 1988. The metabolism and pharmacokinetics of amlodipine in humans and animals. J. Cardiovasc. Pharmacol. 12, S55–S59.
Tenjarla, S.N., Allen, R., Borazani, A., 1994. Evaluation of verapamil hydrochloride permeation through human cadaver skin. Drug Dev. Ind. Pharm. 20, 49–63.
Valiverti, S., Hammell, D.C., Paudel, I.S., Hamad, M.O., Crooks, P.A., Stinchcomb, A.L., 2005. In vivo evaluation of 3-alkyl ester transdermal prodrugs of naltrexone in hairless guinea pigs. J. Control. Release 102, 509–520.
Zhang, X.P., Loke, K.E., Mital, S., Chahwala, S., Hintze, T.H., 2002. Paradoxical release of nitric oxide by an L-type calcium channel antagonist, the R+ enantiomer of amlodipine. J. Cardiovasc. Pharmacol. 39, 208–214.